This is a previous version of the article published in Mathematical Methods in the Applied Sciences. 2021, 44(1): 993-1002. https://doi.org/10.1002/mma.6806

Received: 00 Month 0000 | Revised: 00 Month 0000 | Accepted: 00 Month 0000

DOI: xxx/xxxx

ARTICLE TYPE

Limiting curves in an axially symmetric galaxy

Juan F. Navarro

[1]Department of Applied Mathematics, University of Alicante, Carretera San Vicente del Raspeig s/n 03690 San Vicente Comunidad Valenciana, Spain

Correspondence
*Juan F. Navarro. University of Alicante, Carretera San Vicente del Raspeig s/n, 03690 San Vicente, Alicante, Spain Email: jf.navarro@ua.es

The aim of this article is to reveal the geometry of the windows through which stars escape from a potential modeling the central part of galaxy with axial symmetry and presenting one exit channel. This study has been performed by analyzing the ingoing and outgoing asymptotic orbits to the Lyapunov orbit located at the opening of the potential in a suitable surface of section.

KEYWORDS:
Limiting Curves, Galactic potentials, Escapes, Asymptotic orbits

1 | INTRODUCTION

The phenomenon of escape of stars from an open Hamiltonian system is a widely studied problem.[1,2,3,4,5,6,7,8,9,10,11,12,13,14,15,16] In a galactic potential, the curve of zero velocity opens when the energy of the system is above the escape energy. Then, particles can escape from the potential well through one of the openings of the potential. The escape of a particle from the system can only occur if the particle crosses a particular periodic orbit situated at any opening of the potential. These periodic orbits, known as Lyapunov orbits, are highly unstable and can be considered as the guardians of the escape from the system. The asymptotic curves to them constitute the “limiting curves" of the escape in the phase space. Orbits with initial conditions in the stable manifold to one Lyapunov orbit tend asymptotically to this orbit, and never escape from the system. A small deviation outwards in the initial condition of the orbit gives rise to escape, but if the deviation is produced inwards, then the orbit remains trapped in the potential well. Contopoulos[7] performed an exploration of the escape from a dynamical system representing the central part of a galaxy presenting four openings to infinity. In his analysis, Contopoulos found that the manifolds to the Lyapunov orbits rotate infinitely around some limiting structures. The ratio of orbits leaving the potential well through each of the openings depends on the shape of these asymptotic trajectories related to the Lyapunov orbits. Navarro and Henrard[10] also studied this galactic potential, giving details on the relation between heteroclinic orbits and the infinite spiraling described by Contopoulos, and clarifying that there are an infinite number of spirals, embedded one inside eech other following a “Russian dolls" structure. This same principle rules the escape to infinity in a harmonic oscillator with double symmetry and presenting quartic perturbing terms.[11] In a recent paper, Navarro[12] examine the architecture of this intricate structure of infinite spirals in a galactic potential with two exit channels.

In this paper, we investigate the geometry of the limiting curves of the escape domains in a galactic type potential with axial symmetry by using a suitable selected surface of section. First, we show how the escape domains are distributed in the surface of section. Then, we calculate the asymptotic orbits to the Lyapunov orbit at the opening of the potential, to unveil the way in which these structures rule the escape from the galactic potential. We also give details about the form of the limiting curves of the escape regions, and will describe how they evolve by making use of a new notation to refer to the successive crossings of the asymptotic orbits to the Lyapunov orbit with an adequate surface of section.

2 | THE EQUATIONS OF MOTION

Let us introduce a galactic system modeled by the effective potential

$$W(r,z) = -\frac{L_z^2}{2r^2} - V(r,z)\,, \tag{1}$$

where $V(r,z)$ is the potential

$$V(r,z) = \frac{\omega^2}{2}(r^2+z^2) - \mu\left(\alpha(r^4+z^4) + 2\rho r^2 z^2\right)\,. \tag{2}$$

In (2), r and z are cylindrical coordinates, and ω, μ, α and ρ are parameters. This galactic potential can only model the local motion of a star at short distances from the center of the galaxy ($r_{max} \leq 1.5$ kpc). This is due to the fact that alternatively the mass density grows in an outwardly dirrection from the center, a fact that is not usual in the observed galaxies. Thus, we investigate the escape from the centre of a galactic potential. In 2012, Zotos [14] performed a numerical examination of this potential.

The Hamiltonian associated to the potential (1) reads

$$H = \frac{1}{2}(\dot{r}^2+\dot{z}^2) - W(r,z)\,, \tag{3}$$

that is

$$H = \frac{1}{2}(\dot{r}^2+\dot{z}^2) + \frac{\omega^2}{2}(r^2+z^2) - \mu\left(\alpha(r^4+z^4) + 2\rho r^2 z^2\right) + \frac{L_z^2}{2r^2}\,, \tag{4}$$

and the equations of motion are given by

$$\begin{aligned} \ddot{r} &= \frac{\partial W}{\partial r} = W_r = -\omega^2 r + 4\mu\alpha r^3 + 4\mu\rho r z^2 + \frac{L_z^2}{r^3}\,, \\ \ddot{z} &= \frac{\partial W}{\partial z} = W_z = -\omega^2 z + 4\mu\alpha z^3 + 4\mu\rho r^2 z\,. \end{aligned} \tag{5}$$

In this formalization, we use a system of units in which 1 kpc is the unit of length and 10^7 yr is the unit of time.

There is a critical value of the energy, called escape energy and denoted by H_c, such that for values of the energy beyond H_c, the curves of zero velocity open up to infinity and stars may leave the potential well. If the energy of the system exceeds H_c, then an unstable periodic orbit located across the opening rules the escape from the potential (see right panel of Figure 1). Orbits that go across this orbit from inside of the potential escape to infinity.

The curves of zero velocity are defined by

$$H = \frac{L_z^2}{2r^2} + \frac{\omega^2}{2}(r^2+z^2) - \mu\left(\alpha(r^4+z^4) + 2\rho r^2 z^2\right)\,. \tag{6}$$

Throughout this research, we take $\omega = 1$ $(10^7$ yr$)^{-1}$, $\mu = 1$ $(10^7$ yr kpc$)^{-2}$, $\alpha = 0.2$, $\rho = -1.2$ and $L_z = 0.1$. For these values, the escape energy is given by $H_c = 0.3125$. Figure 1 (left panel) exhibits the curves of zero velocity for three different values of the energy. The size of the opening of the potential grows with the value of the energy. In the right panel of Figure 1 , we show the curve of zero velocity for $H = 0.32$, together with the Lyapunov orbit.

3 | BASINS OF ESCAPE

The set of initial conditions of the escaping orbits composes the so-called “basins of escape". The fractal nature of these domains lies in the geometry of the asymptotic curves to the Lyapunov orbit. In this section, we calculate this set of initial conditions. The initial conditions have been chosen in the surface of section defined by $r = \bar{r} = 0.6$, $\dot{r} > 0$. If we substitute $r = 0.6$, $\dot{r} = 0$ into equation (3), we obtain the limiting curve in the $z - \dot{z}$ plane. This limiting curve corresponds to

$$2H = \dot{z}^2 + \omega^2(\bar{r}^2+z^2) - 2\mu\left(\alpha(\bar{r}^4+z^4) + 2\rho\bar{r}^2 z^2\right) + L_z^2/\bar{r}^2\,. \tag{7}$$

The value of $\dot{r} > 0$ is calculated from the equation (4),

$$\dot{r} = +\sqrt{2H - \dot{z}^2 - \omega^2(\bar{r}^2+z^2) + 2\mu\left(\alpha(\bar{r}^4+z^4) + 2\rho\bar{r}^2 z^2\right) - L_z^2/\bar{r}^2}\,. \tag{8}$$

For the computation of the basins of escape, we integrate 1024×1024 initial conditions chosen to sample uniformly the interior of the squares $[-0.4, 0.4] \times [-0.6, 0.6]$, $[-0.12, 0.12] \times [-0.15, 0.15]$ and $[-0.14, -0.04] \times [0, 0.15]$ in the plane $z - \dot{z}$. As our main purpose is to analyze the connection between the basins of escape and the asymptotic trajectories to the Lyapunov orbit,

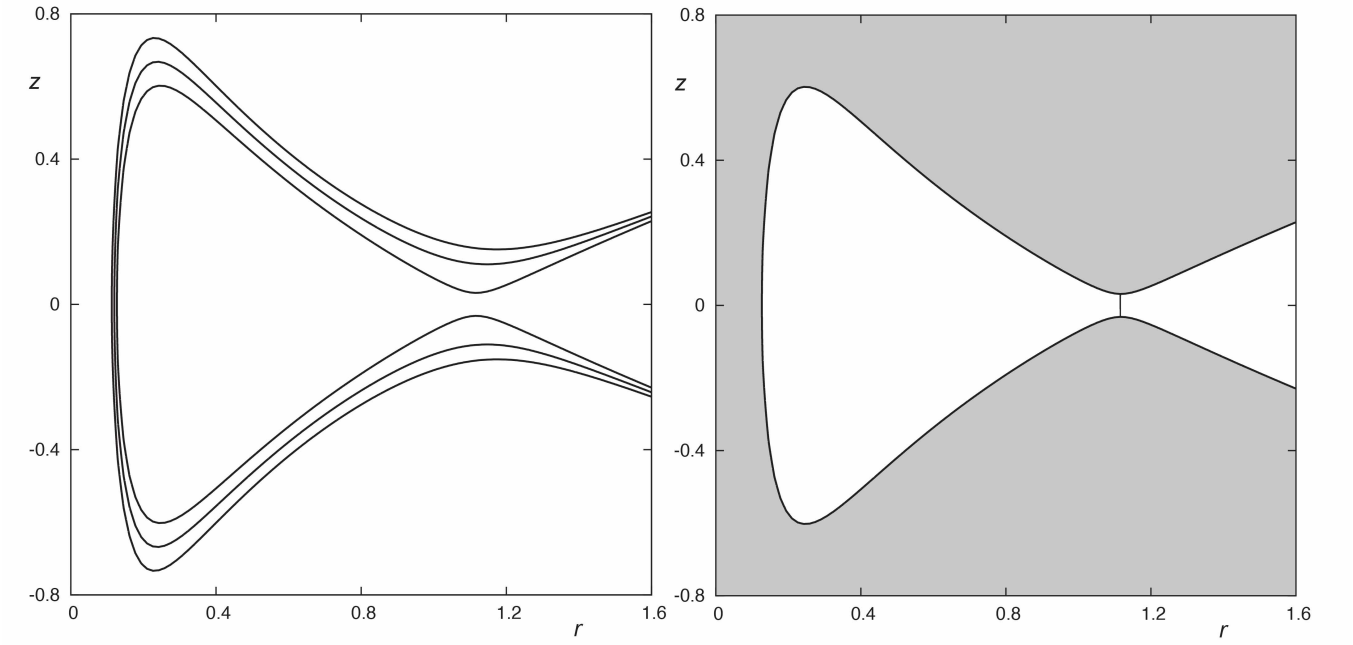

FIGURE 1 Curves of zero velocity for $\omega = 1$, $\mu = 1$, $\alpha = 0.2$, $\rho = -1.2$, $L_z = 0.1$ and several values of the energy larger than the escape energy: $H_1 = 0.32$, $H_2 = 0.36$ and $H_3 = 0.4$ (left panel). In the right panel, we also depict the Lyapunov orbit at the opening of the potential.

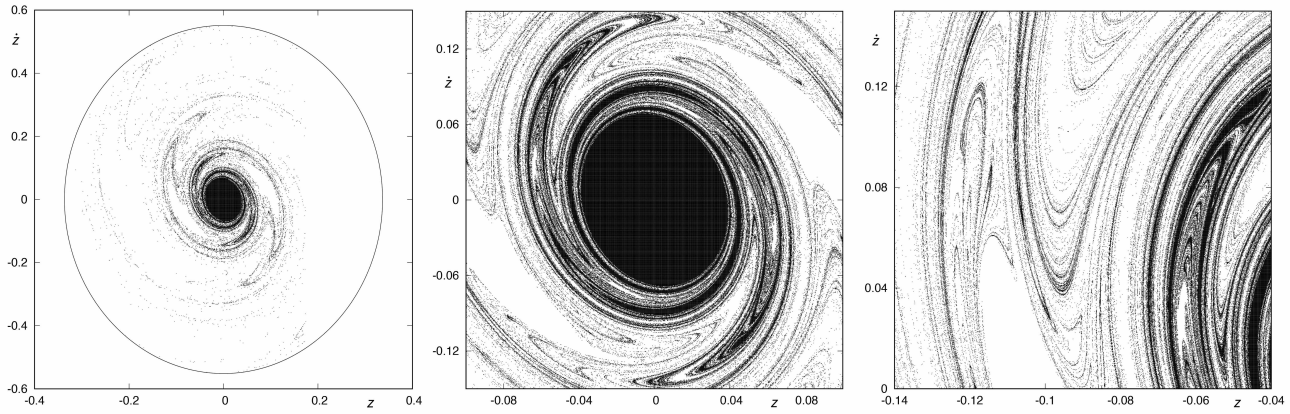

FIGURE 2 Basins of escape for sets of initial conditions uniformly distributed in the squares defined by $[-0.4, 0.4]\times[-0.6, 0.6]$ (left panel), $[-0.12, 0.12] \times [-0.15, 0.15]$ (center panel) and $[-0.14, 0.04] \times [0, 0.15]$ (right panel) in the z-$\dot{z}$ plane.

we adopt the following criterion: the maximum time of numerical integration is defined by $T_e = 10^2$. We consider that a particle escape from the galactic potential if $r > r_e$, where $r_e = 1.2$ has been taken sufficiently large to guarantee that the particle leaves the central part of the galaxy and never returns. If the particle stays inside the domain defined by the curve of zero velocity after T_e units of time, we consider that the orbit is a non-escaping orbit. The numerical integration of the equations of motion has been performed by using recurrent power series, and the accuracy of the numerical solutions has been computed fixed to 10^{-21}.[18]

In Figure 2 , we show the basins of escape by taking three different sets of 1024×1024 initial conditions uniformly spaced in the squares defined by $[-0.4, 0.4] \times [-0.6, 0.6]$, $[-0.12, 0.12] \times [-0.15, 0.15]$ and $[-0.14, 0.04] \times [0, 0.15]$ in the z-$\dot{z}$ plane. In the left panel of Figure 2 , we have also shown the limiting curve given by (7) as well as the basins of escape.

4 | COMPUTATION OF THE ASYMPTOTIC TRAJECTORIES TO THE LYAPUNOV ORBIT

As it has been described above, if the energy of the system exceeds the escape energy then some particles escape to infinity. Located at the aperture of the potential well there is the Lyapunov orbit, which is the guardian of the escape: if an orbit crosses it outwards then escapes from the system. The boundary of the set of escaping orbits is defined by the the orbits tending asymptotically to the Lyapunov orbit from the interior of the potential.[7] For the computation of the initial part of the asymptotic curves to the Lyapunov orbit, we follow the method suggested by Deprit and Henrard.[17] Let us assume that $(r^*(t), z^*(t))$ is a periodic orbit of the equations of motion, with minimal period T. The system is conservative and Hamiltonian, so the set of multipliers of the system is $(+1, +1, \tau, 1/\tau)$, where τ is a nonzero complex number. If τ is real and $|\tau| \neq 1$, Poincaré[19] establishes that the periodic orbit is unstable, and a real number $a > 0$ exists such that $\tau = e^{aT}$. This real number a is known as characteristic exponent of the periodic orbit $(r^*(t), z^*(t))$.

Poincaré showed that to the unstable periodic orbit $\phi(t) = (r^*(t), z^*(t))$, two one-parameter families of orbits are known: one of them tending asymptotically to $\phi(t)$ as $t \to \infty$ (incoming asymptotic orbits), and the other one tending asymptotically to $\phi(t)$ as $t \to -\infty$ (outgoing asymptotic orbits).

Thus, the ingoing asymptotic trajectories to $\phi(t) = (r^*(t), z^*(t))$ of period T are given by the series

$$r(t, \epsilon) = r^*(t) + \epsilon u(t)\,, \quad z(t, \epsilon) = z^*(t) + \epsilon v(t)\,, \tag{9}$$

being

$$\begin{aligned} u(t, \epsilon) &= \sum_{j \geq 1} \epsilon^{j-1} e^{-jat} r_j(t)\,, \\ v(t, \epsilon) &= \sum_{j \geq 1} \epsilon^{j-1} e^{-jat} z_j(t)\,. \end{aligned} \tag{10}$$

For any natural number $j \geq 1$, $r_j(t)$ and $z_j(t)$ are periodic functions with period T. The outgoing asymptotic trajectories are described by analogous series with the exponent $-a$ replaced by $+a$. By making $\epsilon = 0$, we get the periodic orbit back.

It is convenient to fix the following notation: the coefficients

$$u_j(t) = e^{-jat} r_j(t)\,, \quad v_j(t) = e^{-jat} z_j(t)\,, \quad j \geq 1\,,$$

are the Cartesian components of a vector function we refer to as the variation of order j along the periodic orbit $\phi(t)$. Let θ be the inclination of the velocity vector on the r axis. Then, the normal and tangential components (n_j, p_j) of the displacement $u_j, v_j)$ of order j are defined by the identities

$$n_j = -u_j \sin\theta + v_j \cos\theta\,, \quad p_j = u_j \cos\theta + v_j \sin\theta\,, \quad j \geq 1\,.$$

As these relations are linear, the analytical continuation of the family of ingoing asymptotic orbits implies to expanding the normal and tangential components (n, p) of the displacement (u, v) into power series

$$\begin{aligned} n(t, \epsilon) &= \sum_{j \geq 1} \epsilon^{j-1} e^{-jat} n_j(t)\,, \\ p(t, \epsilon) &= \sum_{j \geq 1} \epsilon^{j-1} e^{-jat} p_j(t)\,. \end{aligned} \tag{11}$$

For any $j \geq 1$, the normal and tangential variations are written as

$$n_j(t) = e^{-jat} N_j(t)\,, \quad p_j(t) = e^{-jat} P_j(t)\,, \tag{12}$$

where N_j and P_j are periodic functions in t with period T.

Now, by expanding the functions $W(r^*(t) + u, z^*(t) + v)$, $W_r(r^*(t) + u, z^*(t) + v)$ and $W_z(r^*(t) + u, z^*(t) + v)$ in double series of the components (u, v), we get

$$\begin{aligned} W(r^*(t) + u, z^*(t) + v) &= W(r^*(t), z^*(t)) + uW_r(r^*(t), z^*(t)) + vW_z(r^*(t), z^*(t)) + \bar{W}(u, v, t)\,, \\ W_r(r^*(t) + u, z^*(t) + v) &= W_r(r^*(t), z^*(t)) + uW_{rr}(r^*(t), z^*(t)) + vW_{rz}(r^*(t), z^*(t)) + \bar{W}_r(u, v, t)\,, \\ W_z(r^*(t) + u, z^*(t) + v) &= W_z(r^*(t), z^*(t)) + uW_{zr}(r^*(t), z^*(t)) + vW_{zz}(r^*(t), z^*(t)) + \bar{W}_z(u, v, t)\,, \end{aligned}$$

where $\bar{W}$, $\bar{W}_r$ and $\bar{W}_z$ are power series in u and v beginning with quadratic terms, and with coefficients being functions of t. The substitution of these expressions into equation (5) leads to

$$\begin{aligned} \ddot{u} &= W_{rr}(r^*(t), z^*(t))u + W_{rz}(r^*(t), z^*(t))v + \bar{W}_r\,, \\ \ddot{v} &= W_{zr}(r^*(t), z^*(t))u + W_{zz}(r^*(t), z^*(t))v + \bar{W}_z\,. \end{aligned} \tag{13}$$

From equation (13), we get that the coefficients n_j and p_j of the normal and tangential components (n, p) of the displacement (u, v) must satisfy

$$\ddot{n}_1 + \lambda n_1 = 0\,, \tag{14}$$

$$V\dot{p}_1 - \dot{V}p_1 = 2V\dot{\theta}n_1\,, \tag{15}$$

at the first order and, for any order $j \geq 1$,

$$\ddot{n}_j + \lambda n_j = \Phi_j e^{-jat}\,, \tag{16}$$

$$V\dot{p}_j - \dot{V}p_j = 2V\dot{\theta}n_j + \Psi_j e^{-jat}\,, \tag{17}$$

where

$$\lambda = \frac{\ddot{V}}{V} + 2\dot{\theta}^2 - W_{rr} - W_{zz}\,,$$

V is the velocity along the orbit, and Φ_j and ψ_j are periodic functions of t with period T. The key point is to expand in an automatic way the functions $\bar{W}$, $\bar{W}_r$ and $\bar{W}_z$ in power series of ϵ. The most straightforward procedure is to expand them recursively in power series of ϵ without intermediate development in powers of u and v. Let us assume that the construction of the series (11) has been completed up to order $k-1$. The algorithm enters order k by setting the unknown variations n_j and p_j equal to zero. Then, using the relations

$$u_j = p_j \cos\theta - n_j \sin\theta\,, \quad v_j = p_j \sin\theta + n_j \cos\theta\,,$$

we obtain the variations (10) as power series of ϵ. The Cartesian components u_k and v_k of the variations of order k are provisionally set to zero until they are computed. Now, we can compute the coefficients of ϵ^k in the various functions of r and z which enter W, W_r and W_z. The convention that u_k and v_k be kept equal to zero as long as they have not been computed has the effect that the calculations just performed have produced the coefficients of ϵ^k in the series $\bar{W}$, $\bar{W}_r$ and $\bar{W}_z$. As these coefficients contain e^{-kat}, we have now obtained the periodic functions Φ_k and Ψ_k in the right-hand member of the system (16).

Actually, it is not essential to know Φ_k and Φ_k explicitly as functions of time because we must interpolate them in Fourier series. Thus, we only need to calculate them at uniformly spaced instants of time along the period. This can be performed by funding at each time $\bar{t}$ the coefficients of ϵ^k in the series $W(r(\bar{t}), z(\bar{t}))$, $W_r(r(\bar{t}), z(\bar{t}))$ and $W_z(r(\bar{t}), z(\bar{t}))$, hence the numerical values at $\bar{t}$ of the right-hand members of system (16) and, after dividing by $e^{-ja\bar{t}}$, those of $\Phi_k(\bar{t})$ and $\Psi_k(\bar{t})$.

5 | THE BOUNDARIES OF THE ESCAPE WINDOWS

The asymptotic manifolds to the Lyapunov orbit cross a surface of section along a closed curve, which is called "limiting asymptotic curve". For a precise determination of the frontiers of the windows of escape, we have integrated backward a set of 1 000 000 initial conditions located at the ingoing asymptotic trajectories to the Lyapunov orbit, up to their intersection with the surface of section defined by $r = \bar{r} = 0.6$ ($\dot{r} > 0$). The computation of this set of initial conditions of the stable manifold have been performed by fixing the value of $\epsilon \exp(at)$ to 10^{-4}, and selecting 1 000 000 equally spaced values of the initial time t.

To ease the analysis of the consecutive collection of crossings of the limiting asymptotic curves with the surface of section, we introduce the following notation. Let ϕ be the Lyapunov orbit at the opening of the galactic potential. Then, $W_{s,\nu}(\phi)$ denotes the ν-th crossing of the ingoing asymptotic orbits to ϕ with the surface of section $r = \bar{r}$, and $W_{u,\nu}(\phi)$ the ν-th crossing of the outgoing asymptotic orbits with the surface of section $r = \bar{r}$. Here, $\nu \in \mathbb{N}$.

Figure 3 exhibits the first crossing of the ingoing asymptotic orbits to $\phi(t)$ with $r = \bar{r}$ ($\dot{r} > 0$), that is, $W_{s,1}(\phi)$. The first crossing of the outgoing asymptotic orbits with $r = \bar{r}$ takes place for $\dot{r} < 0$, so these two sets do not intersect:

$$W_{s,1}(\phi) \cap W_{u,1}(\phi) = \emptyset\,.$$

Orbits starting inside $W_{s,1}(\phi)$ escape directly through the opening of the potential, while orbits with initial conditions inside the area eclosed by $W_{u,1}(\phi)$ come from infinity.

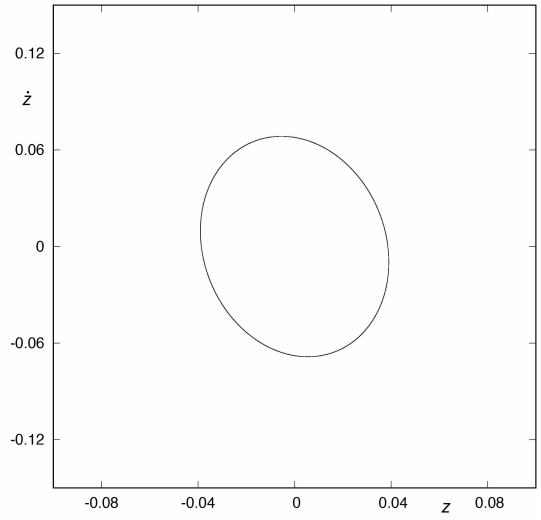

FIGURE 3 $W_{s,1}(\phi)$: first crossing of the ingoing asymptotic orbits to $\phi(t)$.

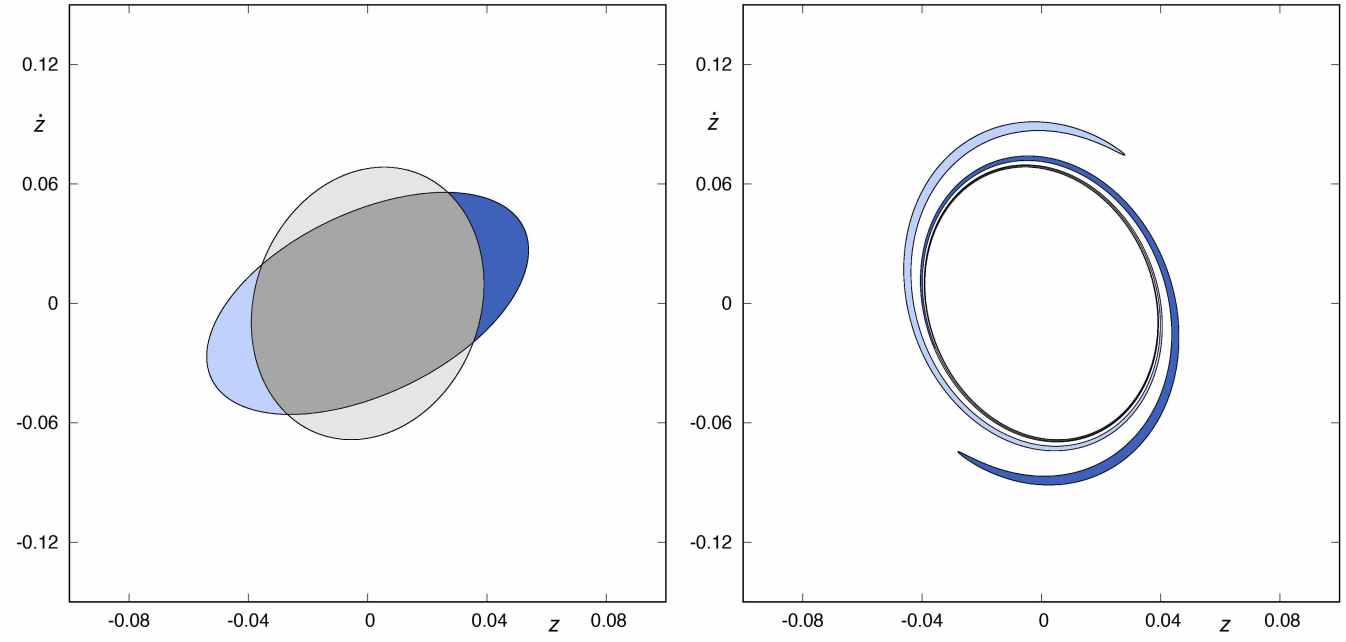

FIGURE 4 In the left panel, intersection between $W_{s,2}(\phi)$ and $W_{u,1}(\phi)$ (in grey). In the right panel, $W_{s,3}(\phi)$.

The second crossing of the ingoing asymptotic orbits to $\phi(t)$ with the surface of section $r = \bar{r}$ occurs for $\dot{r} < 0$. Figure 4 (left panel) shows the intersection between $W_{s,2}(\phi)$ and $W_{u,1}(\phi)$. Both sets intersect at four points corresponding to four homoclinic orbits to the Lyapunov orbit. These homoclinic orbits cross the surface of section defined by $r = \bar{r}$ at two different instants of time. Figure 5 (left panel) shows one of these homoclinic orbits.

Orbits with initial conditions inside the domain limited by both crossings ($W_{s,2}(\phi)$ and $W_{u,1}(\phi)$), colored in dark grey in Figure 4 , are coming from the infinity and leave the central part of the galaxy after crossing the surface of section $r = \bar{r}$ at two different instants of time. In the right panel of Figure 5 (right panel), we depict one of these orbits. Furthermore, orbits with initial conditions inside one of the two “tongues" colored in blue in left panel of Figure 4 , have a preceding crossing with the surface of section $r = \bar{r}$, and certainly leave the galaxy in the future by the opening to infinity.

The third crossing of the ingoing asymptotic orbits to ϕ, depicted in the right panel of Figure 4 , is constituted of two “tongues" which tend infinitely spiraling to the first crossing of the ingoing asymptotic orbits to ϕ, $W_{s,1}(\phi)$. These two tongues are the

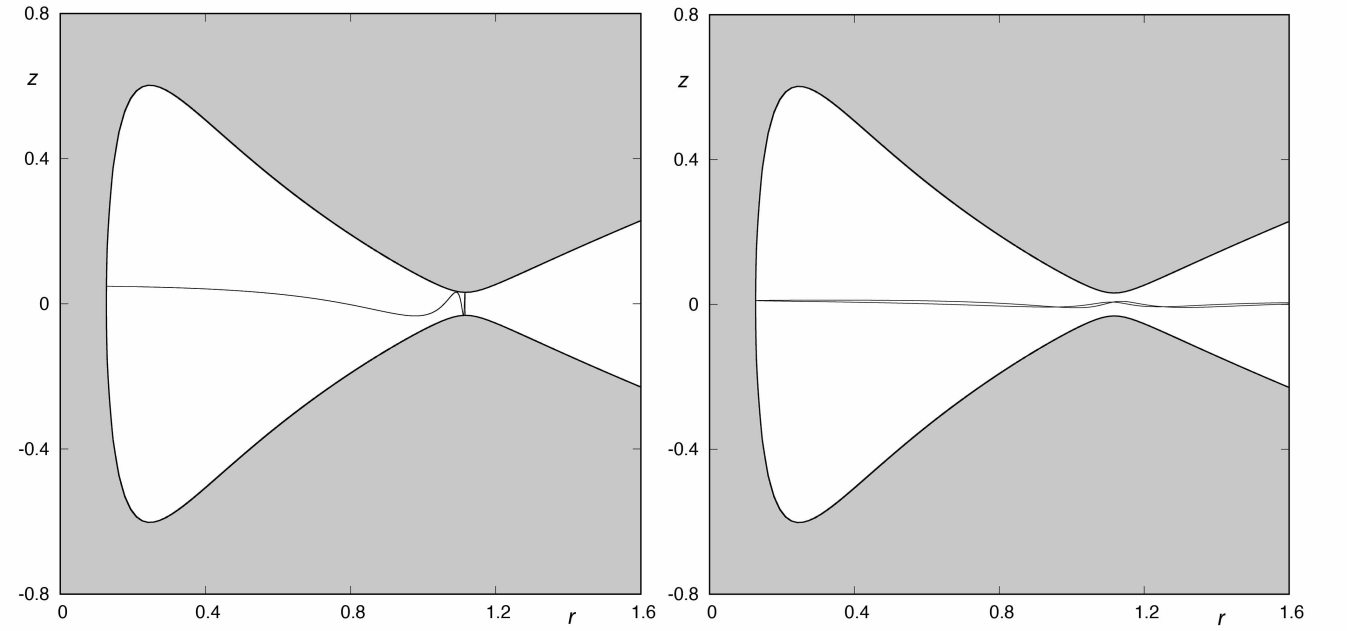

FIGURE 5 In the left panel, homoclinic orbit intersecting two times the surface of section $r = \bar{r}$. In the right panel, an orbit coming from infinity and leaving the potential well after intersecting two times the surface of section.

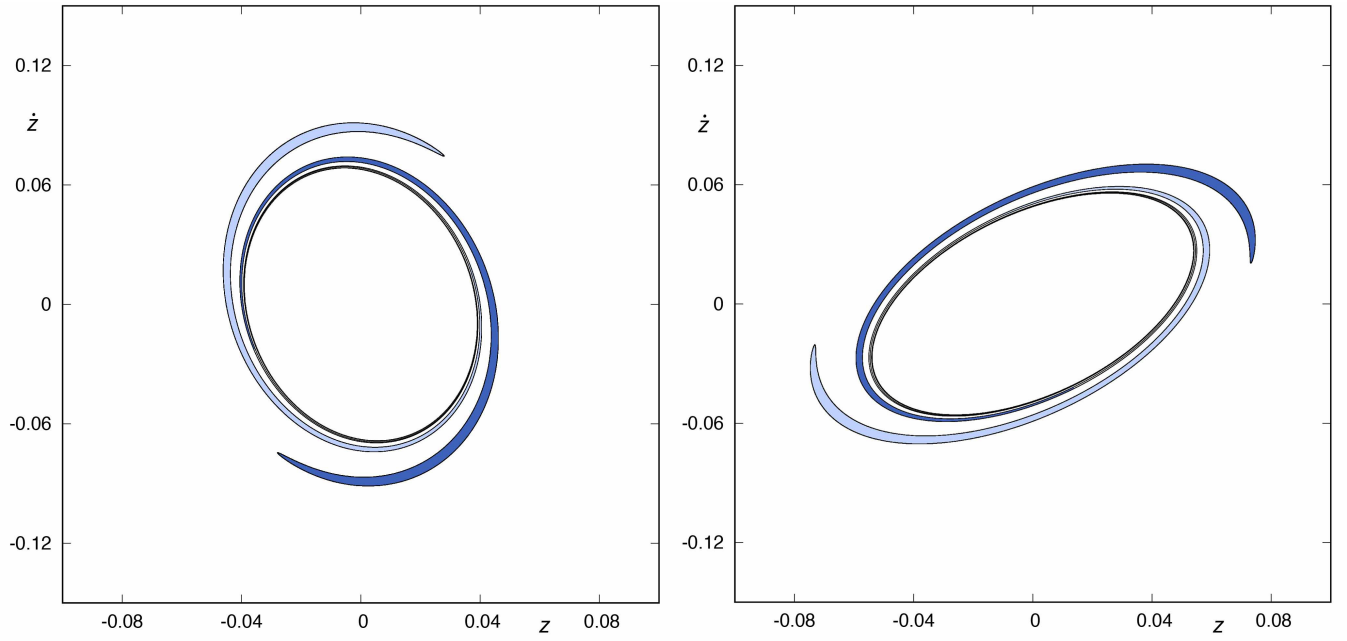

FIGURE 6 $W_{s,3}(\phi)$ (left panel) and $W_{s,4}(\phi)$ (right panel).

antecedents of the two tongues colored in blue in the left panel of Figure 4 . The crossing $W_{s,3}(\phi)$ occurs with $\dot{r} > 0$, so it does not intersect $W_{u,1}(\phi)$. Consequently, all the orbits with initial conditions in the inside of these two tongues have a precedent crossing with the surface of section $r = \bar{r}$, and will leave the galaxy by the opening of the potential after two crossings with the surface $r = \bar{r}$. Therefore, the fourth crossing of the ingoing asymptotic orbits to $\phi(t)$ with the surface of section $r = \bar{r}$, is also made up of two tongues, with a structure infinitely spiraling around $W_{s,2}(\phi)$. In Figure 6 (right panel), we can observe the fourth crossing of the ingoing asymptotic orbits to ϕ with the surface of section. As it happens in the third crossing, orbits with

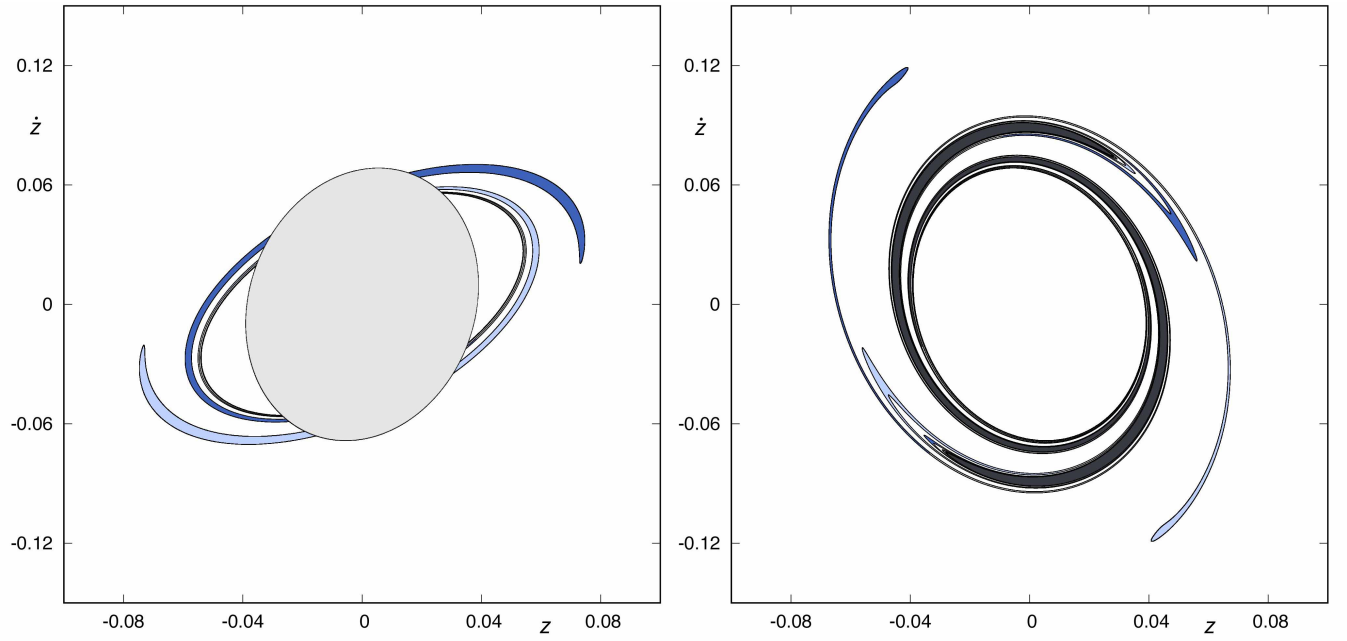

FIGURE 7 Intersection between $W_{s,4}(\phi)$ and $W_{u,1}(\phi)$ (left panel), and $W_{s,5}(\phi)$ (right panel).

initial conditions inside one of the two tongues will go away from the galactic potential by the opening guarded by the Lyapunov orbit after intersecting the surface of section $r = \bar{r}$ at three different instants of time. The two tongues composing $W_{s,4}(\phi)$ are the images of the two tongues of $W_{s,3}(\phi)$ colored in blue in Figure 6 (left panel).

In Figure 7 (left panel), we depict the intersection between $W_{s,4}(\phi)$ and $W_{u,1}(\phi)$. These two sets intersect at an infinite set of points. Each of these points corresponds to a homoclinic orbit to ϕ which crosses the surface of section $r = \bar{r}$ at four different instants of time. We exhibit a homoclinic orbit of this type in the left panel of Figure 8 . Orbits with initial conditions in the interior of $W_{1,u}(\phi)$ and one of the two tongues of $W_{s,4}(\phi)$, enter the galaxy from the infinity by the opening of the potential and escape by the same window after crossing the surface $r = \bar{r}$ at four different instants of time. In Figure 8 , we show an orbit of such a type. Orbits with initial conditions in the inner part of the tongues and outside the grey area enclosed by $W_{u,1}(\phi)$ have a preceding crossing in the surface of section. In the right panel of Figure 7 , we can observe the fifth intersection of the stable manifold with the surface of section.

It is easier to understand the geometry of $W_{s,5}(\phi)$ by analyzing how the two basic types of structures that appear in the intersection between $W_{u,1}$ and $W_{s,2n}$ are transformed when we follow them backward until they intersect again the surface of section, for any $n \in \mathbb{N}$. In particular, we are interested in the part of the area enclosed by $W_{s,2n}$ which is outside $W_{u,1}$. The first type of structure is called “tongue", and we have colored the scheme of one of them in blue in the left panel of Figure 9 . There, we can observe that $W_{s,2n}$ cuts $W_{u,1}$ at two points. Each point of intersection corresponds to a homoclinic orbit which cross the surface of section defined by $r = \bar{r}$ at $2n$ different instants of time. The blue area in the left panel of Figure 9 has a preceding crossing with the surface of section. When we follow this set of initial conditions backward, we get the blue tongue infinitely spiraling around $W_{s,2n-1}$ represented in the right panel of Figure 9 .

The second type of structure is called “bridge", and we have represented an scheme of one of them in the left panel of Figure 10 . As we can see in that panel, $W_{u,1}$ intersects $W_{s,2n}$ at four points. Each of these points corresponds to a homoclinic orbit which crosses the surface of section at $2n$ different instants of time. The blue area in the left panel of Figure 9 has a previous intersection with the surface of section. When we follow this set of initial conditions backward, we get the blue bridge infinitely spiraling around $W_{s,2n-1}$, represented in the right panel of Figure 9 in light brown color.

Finally, Figure 11 shows a detail of the escape basins in the $z - \dot{z}$ plane (left panel), as well as the set $W_{s,17}(\phi)$. We observe clearly how the limit curve of the basins of escape is the projection of the stable manifold to the Lyapunov orbit in the $z - \dot{z}$ plane.

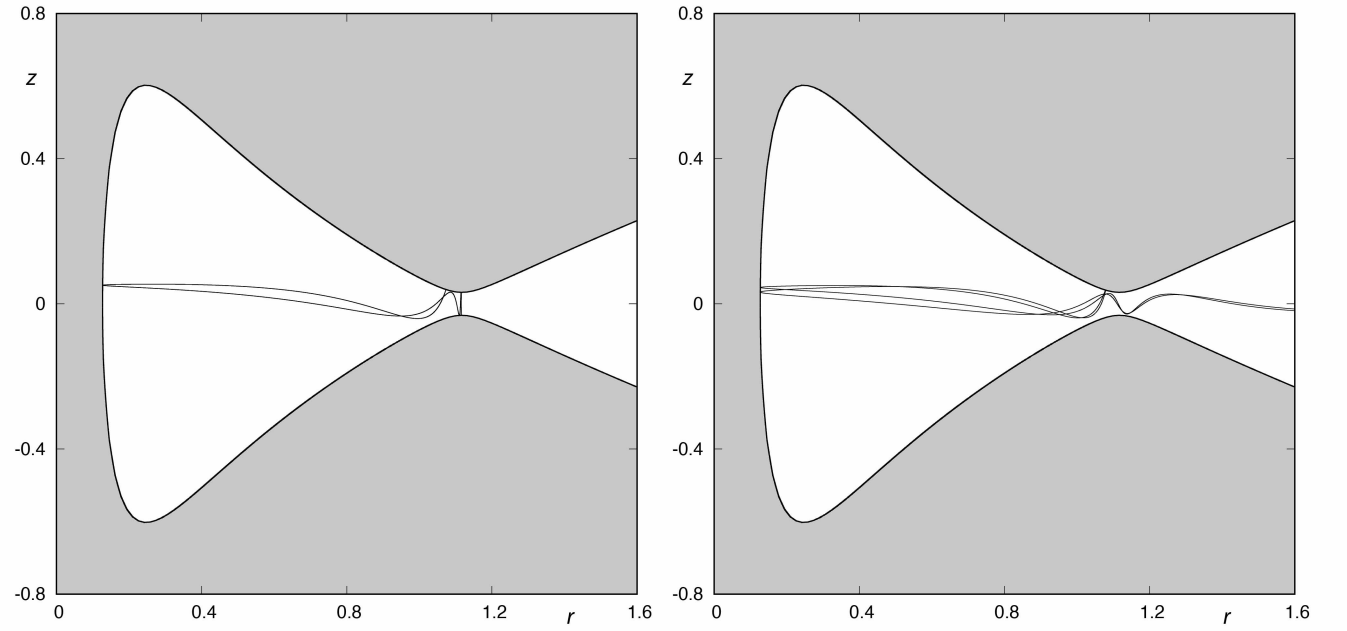

FIGURE 8 In the left panel, homoclinic orbit intersecting four times the surface of section $r = \bar{r}$. In the right panel, an orbit coming from infinity and leaving the potential well after intersecting four times the surface of section.

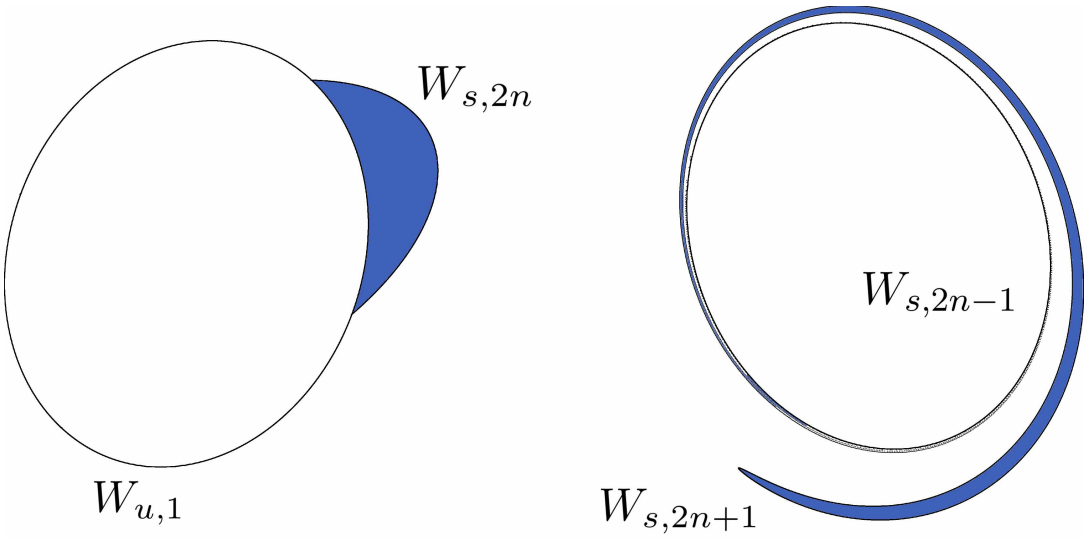

FIGURE 9 Illustration of the pre-image of a tongue. In the left, we show $W_{u,1}(\phi)$ and a tongue belonging to $W_{s,2n}$ outside the area covered by $W_{u,1}$ in the surface of section. In the right, the pre-image of this tongue, $W_{s,2n+1}$, a tongue infinitely spiraling arounf $W_{s,2n-1}$. Here, $n \in \mathbb{N}$.

6 | CONCLUSIONS

In a galactic potential, the curve of zero velocity opens when the energy of the system is above the escape energy. Then, particles can escape from the potential well through one of the openings of the potential. The escape of a particle from the system can only occur if the particle crosses a particular periodic orbit located at any opening of the potential. These periodic orbits, called Lyapunov orbits, are highly unstable and can be considered as the guardians of the escape from the system. The asymptotic

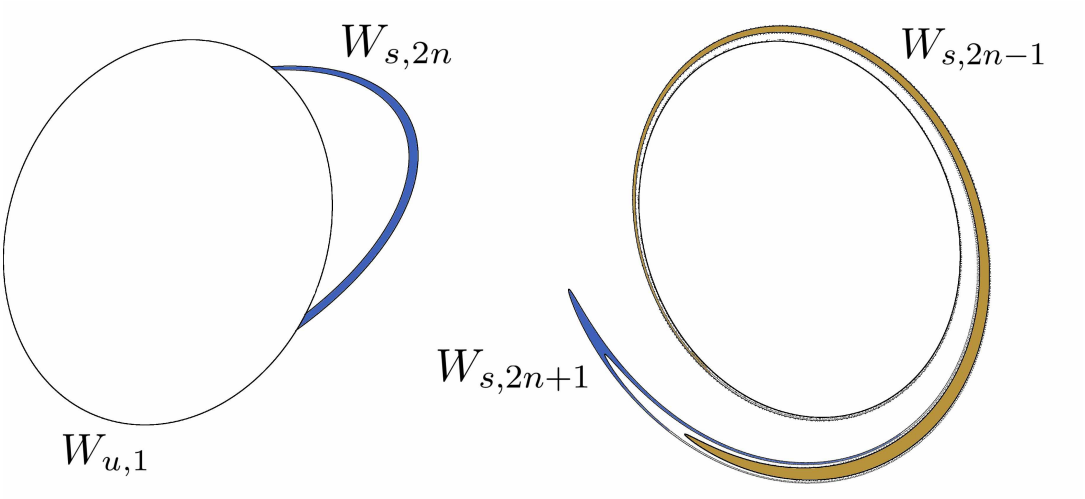

FIGURE 10 Illustration of the pre-image of a bridge. In the left, we show $W_{u,1}(\phi)$ and a bridge (in blue) belonging to $W_{s,2n}$ outside the area covered by $W_{u,1}$ in the surface of section. In the right, the pre-image of this bridge, $W_{s,2n+1}$, a bridge (also in blue) infinitely spiraling arounf $W_{s,2n-1}$ (in light brown). Here, $n \in \mathbb{N}$.

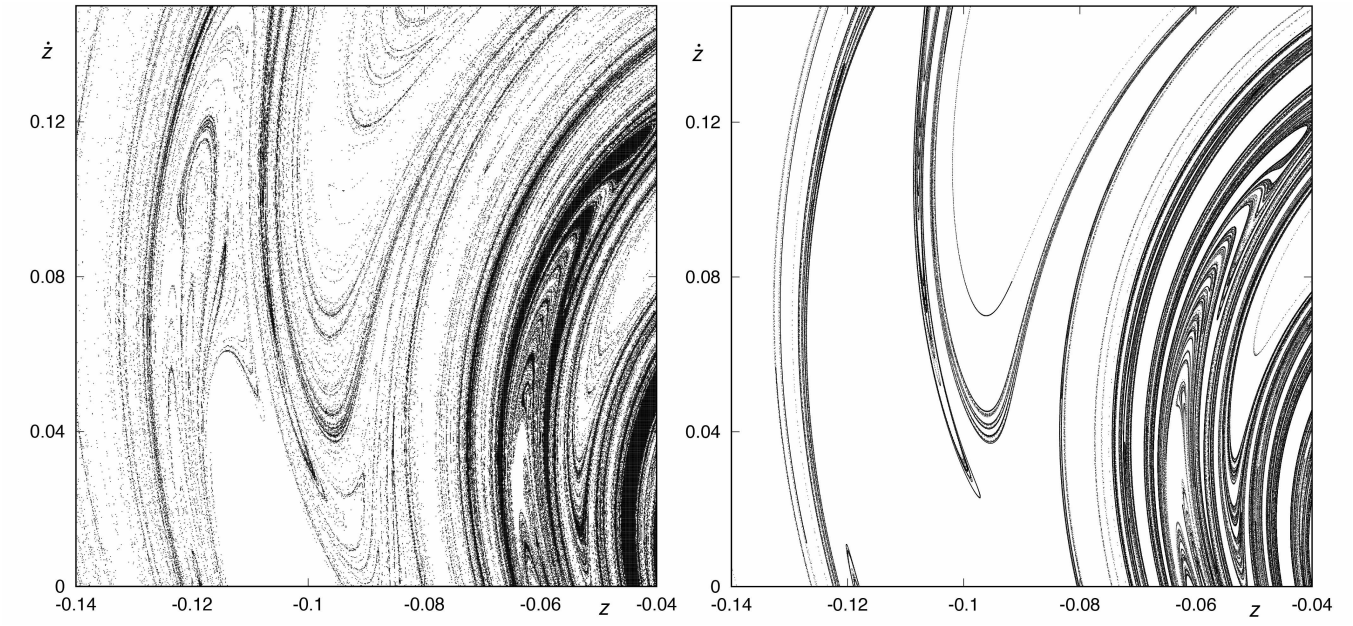

FIGURE 11 Portrait of a detail of the basins of escape (left panel). Black points correspond to orbits that escape to infinity by the opening of the potential, and $W_{s,17}(\phi)$ (right panel).

curves to them constitute the “limiting curves" of the escape in the phase space. In this paper, we have computed these limiting curves, showing that, in fact, they surround the basins of escape of the system.

Conflict of interest

This work does not have any conflicts of interest.

References

1. Aguirre J, Vallejo JC, Sanjuan MAF. Wada basins and chaotic invariant sets in the Hénon–Heiles system. *Phys Rev E*. 2001;64:066208.
2. Aguirre J, Sanjuan MAF. Limit of small exits in open Hamiltonian systems. *Phys Rev E*. 2003;67:056201.
3. Aguirre J, Viana RL, Sanjuan MAF. Fractal structures in nonlinear dynamics. *Rev Mod Phys*. 2009;81:333-386.
4. Barbanis B. Escape regions of a quartic potential. *Celest Mech Dyn Astron*. 1990;48(1):57-77.
5. Barrio R, Blesa F, Serrano S. Fractal structures in the Hénon–Heiles Hamiltonian. *Europhys Lett*. 2008;82:10003.
6. Barrio R, Blesa F, Serrano S. Bifurcations and safe regions in open Hamiltonians. *New Journal of Physics*. 2009;11:053004.
7. Contopoulos G. Asymptotic curves and escapes in Hamiltonian systems. *Astron Astrophys*. 1990;231(1):41-45.
8. Contopoulos G, Kaufmann D. Types of escapes in a simple Hamiltonian system, *Astron Astrophys*. 1992;253(2):379-388.
9. De Moura APS, Letelier PS. Fractal basins in Henon-Heiles and other polynomial potentials. *Phys Lett A*. 1999;256:362-368.
10. Navarro JF, Henrard J. Spiral windows for escaping stars. *Astron Astrophys*. 2001;369:1112-1121.
11. Navarro JF. Windows for escaping particles in quartic galactic potentials. *Applied Mathematics and Computation*. 2017;303:190-202.
12. Navarro JF. On the escape from potentials with two exit channels. *Scientific Reports*. 2019;9:13174:1-17.
13. Siopsis C, Kandrup HE, Contopoulos G, Dvorak R. Universal properties of escape in dynamical systems. *Celest Mech Dyn Astron.* 1996;65(1-2):57-68.
14. Zotos EE. Trapped and escaping orbits in an axially symmetric galactic-type potential. *PASA*. 2012;29:161-173.
15. Zotos EE. Escape dynamics in a Hamiltonian system with four exit channels. *Nonlinear Studies*. 2015;22(3):1-20.
16. Zotos EE. Escape and collision dynamics in the planar equilateral restricted four-body problem. *International Journal of Non-Linear Mechanics* 2016;86:66-82.
17. Deprit A, Henrard J. Construction of orbits asymptotic to a periodic orbit, *Astron J*. 1969;74:308-316.
18. Navarro JF. On the integration of an axially symmetric galaxy model, *Comp and Math Methods*. 2019;1:e1062:1-14.
19. Poincaré H. *Les Methodes Nouvelles de la Mécanique Celeste I*. Paris: Gauthiers–Villars; 1892.